

# The WFC3 IR “Blobs”

---

N. Pirzkal, A. Viana, A. Rajan  
Apr 26, 2010

---

## ABSTRACT

*Small blemishes have been appearing in WFC3 IR images. These blemishes are regions of effectively lowered (by ~10-15%) sensitivity. Following the discovery of these “Blobs” in IR WFC3 observations, we have performed a systematic search for them and have been monitoring all new WFC3 IR data for the appearance of new Blobs. Using data covering the past few months, we have been able to assemble an exhaustive list of their positions and sizes as well as other physical properties.*

*In this ISR, we describe the physical properties of Blobs in two bandpasses (F125W and F160W), and summarize tests that we have performed to ascertain that these are physically located on the Control Select Mechanism (CSM) mirror itself and not on the IR detector. We also show that, while the number of Blobs increased quickly immediately after WFC3 was installed on board of HST, they now appear at a much reduced rate of less than 1 per month. We have currently identified a total of 18 Blobs. These artifacts affect only a small fraction, or ~1.2%, of WFC3 IR pixels. They are small, with radii of ~10--15 pixels, and stable, so that that observers should be able to dither around them to lessen their impact.*

---

## Introduction

WFC3 was installed on board of HST during SM4 in May 2009. Following its installation, some of the images obtained using its IR channel have been affected by a small number of blemishes that appear to have up to 10--15% lower count rates than the surrounding areas. These “Blobs” were not seen or detected during ground testing and have been progressively appearing in IR images obtained after July 2009. They are most visible in images containing a large uniform object, or alternatively images with high background levels. Over the last few months, we have systematically examined all available WFC3 IR data to detect and monitor the Blobs. We have been able to determine their likely cause, and their physical properties, such as positions,

sizes, and depths. We have also been able to determine the rate at which new Blobs appear, and the stability of a Blob once it has appeared.

The purpose of this ISR is to provide observers with a description of what these IR Blobs are and with a list of IR Blobs, since these can impact IR observations requiring accurate photometry.

We summarize our findings about the likely source of these artifacts in Sections 2 and 3, how we identify them and monitor them in Sections 4 and 5, the rate at which they are appearing and their general properties in the F125W and F160W bands in Sections 6 and 7. We conclude by listing the positions of currently known Blobs in the WFC3/IR channel.

## 1. First Detection

The first instance of a Blob was in exposures taken in July 2009, shortly after launch and installation of WFC3 in HST. A round, darker area was readily visible in the pipeline processed FLT files of a few GO datasets. These were not detected in any of the associated and contemporary bias, dark or flat-field calibration files. Further examination of all available WFC3 IR data showed that this artifact likely appeared between July 19, 2009 and August 6, 2009. Another Blob was then observed to have appeared some time between August 6, 2009 and August 8, 2009. In both instances, once a Blob appeared, it remained detectable in all subsequent observations as long as these were deep enough to contain a significant number of IR background photons. In practical terms, this means that Blobs are visible in long exposures, with more than ~300s, broad band filter images. In no cases, and this remains true to this day, has a Blob appeared and then either disappeared, changed its appearance or physically moved in a significant way. As we discuss below, the sizes and position of Blobs have not been changing. The one notable exception being the one described in the following section and that provides us with evidence that Blobs are not artifacts on the WFC3 IR detector itself, but rather originate from particles that have been sticking to the mirror of the Channel Select Mechanism (CSM). The CSM mirror diverts incoming light into the WFC3 IR channel. The CSM moves the mirror out of the way when the UVIS side of WFC3 is used. Chapter 2 of the WFC3 Instrument Handbook describes this in more details and Figure 2.1, in particular, shows the detailed optical layout of the WFC3 instrument.

In Figure 1, we show a single WFC3 IR exposure of a sparse deep field that is long enough to accumulate a significant amount of background flux, and Blobs (shown with red circles) are readily visible. In this figure, we show a few of the known IR Blobs and labeled two of the largest Blobs, located in the bottom left of the field of view. These are measured to attenuate incoming light by 10--15% near their center.

## 2. Blobs and the CSM

Following the identification of Blobs in IR data, they remained at fixed positions in all subsequent IR images, with only one notable exception: On August 28, 2009, the WFC3 CSM was

commanded to switch from the UVIS channel to the IR channel but it failed to reach the exact commanded position. This resulted in a slight shift of the entire field of view on the sky. All sources in the subsequent images were shifted in the same direction (roughly 5 pixels towards the top right corner of the IR detector). The Blobs were seen to be shifted by the same offset and in the same direction. If the Blobs were defects on the detector itself they would not have shifted with the rest of the field. This was a giveaway that Blobs are not located on the WFC3 IR detector but are rather somewhere else in the optical path, likely on the CSM mirror itself.

### 3. CSM Test

The hypothesis that Blobs are caused by defects or particles stuck on the CSM mirror was verified using a short dedicated calibration program (12006, P.I.: Pirzkal). In this program, Stephan's Quartet was observed, providing ample diffuse background, while a set of eight 300s exposures were taken in the F140W filters. Between each exposure, the CSM was commanded to move away, in discrete steps, from its nominal IR position. Images were obtained using CSM offsets of +1, +1+1, +1+4, +4, +10, -10, -5, -3, shifting the field of view towards the top right corner of the field and then shifting it back as the the CSM was brought back to its nominal IR position. The forward and backward offsets were chosen to be different to make sure that the whole system did not suffer from any hysteresis effect and that a single relation between CSM and Blob positions existed. The positions of Blobs were clearly measured to be shifted by 9.9, 19.8, 62.8, 129., 65., and 22.8 pixels, respectively. A summary of the datasets and the relative positions of Blobs is shown in Table 1. In Figure 3, we show the first image minus the second, third and fourth exposures. There, one can see the original Blob (dark spot) and the subsequent position of the same Blob in following exposures (lighter spot). It is difficult to assign an exact center to a Blob as these are somewhat fuzzy in shape but, within the relatively large uncertainties associated with measuring the positions of Blobs in individual images, there appears to be a linear relation between CSM position and position of Blobs in the image. Moreover, as the CSM was brought back to its original position the Blobs also returned to their exact position in the field of view. This can be seen in Figure 4 where we show the first and final images from Table 1 and the difference between these two images. There is no evidence of any shift induced by CSM motion in these images, as demonstrated by the fact that the Blob is not visible in the difference image.

Program 12006 hence confirmed that the WFC3 IR Blobs are likely caused by the CSM mirror itself. We have no reason to believe that these are defects of the mirror coating itself as Blobs appear somewhat fuzzy, and they are more likely caused by material or fibers that have been slowly accumulating onto the mirror. While maybe not statistically significant, the largest Blobs appear to be preferentially located in the bottom left part of the field of view. This would be consistent with small differences in the distance between the CSM mirror and the WFC3 detector itself because the latter would cause material on the CSM mirror to appear more out of focus in the bottom left of the field of view, as we maybe see with Blobs. There does not appear to be a correlation between the frequency of the number of CSM moves (done to switch from the UVIS

to the IR sides of WFC3) and how quickly Blobs have been appearing, as shown in Figure 3. In the latter Figure, we plot the cumulative number of CSM moves as a function of time, and also indicate the cumulative number of Blobs detected, as a function of time.

**Figure 1:** A single WFC3 IR image showing the location of a few IR Blobs. Some of these, like the two bright ones near the top of the bottom left quadrant, labeled 1 and 2, result in a 10% and 5% reduction in the measured count rates in these areas, respectively. The Blobs are not uniform however and their impact on photometry depends on how large of an aperture is used. They attenuate signal more strongly in their centers.

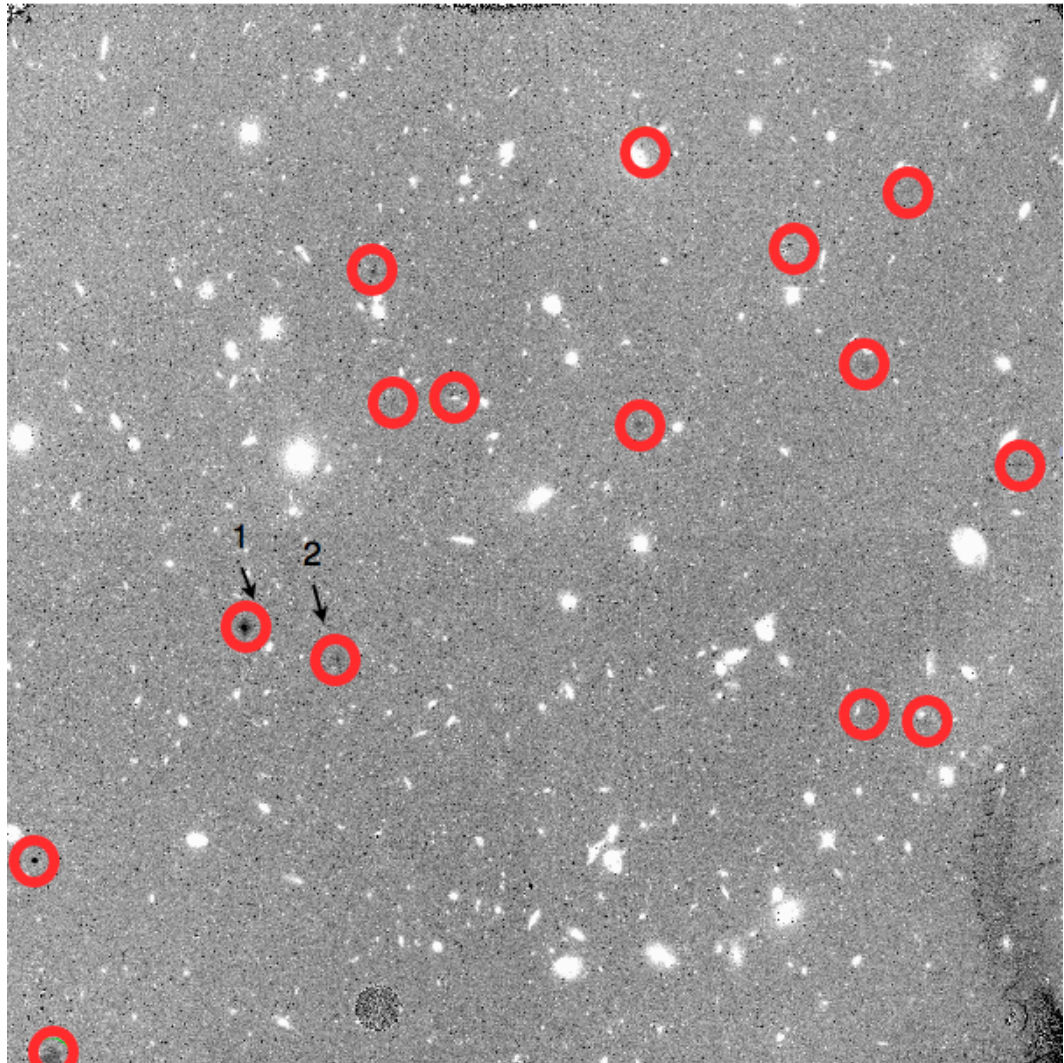


**Figure 2:** The cumulative number of CSM moves from mid-2009 to March, 2010 (blue). We also indicate the cumulative number of Blobs present in images from August, 2009 to March, 2009. While the CSM has continued to be used at a rate of about 500 moves per month, the cumulative number of Blobs has not been increasing in a constant rate.

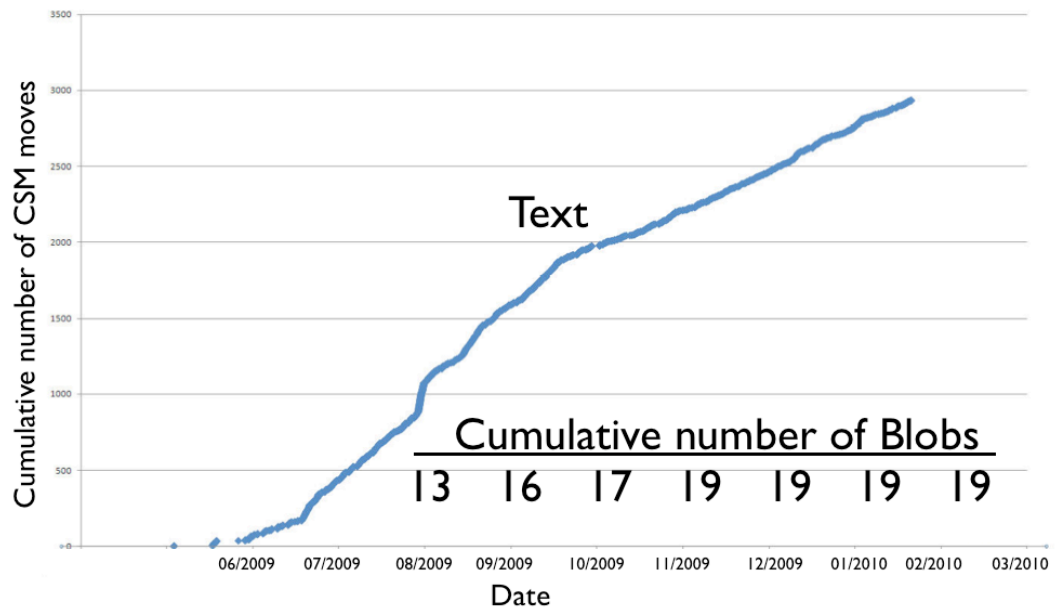


**Table 1:** Datasets observed during the CSM test program 12006. This program purposefully commanded the CSM to move by a series of steps in the positive direction before progressively backtracking to the default IR CSM position.

Dataset	CSM Offset	CSM Relative Position	X (Pixel)	Y (Pixel)	Distance (Pixel)
ibda01q2q	0	0	229	416	0.0
ibda01q3q	+1	1	236	423	9.9
ibda01q5q	+1+1	3	242	431	19.8
ibda01q6q	+1+4	8	267	466	62.8
ibda01q8q	+10	18	304	521	129.0
ibda01qaq	-10	8	268	468	65.0
ibda01qbq	-5	3	243	434	22.8
ibda01qcq	-3	0	229	416	0.0

**Figure 3:** A Blob (Blob 1 in Figure 1) as seen in the difference images between the first and second, first and third and first and fourth images listed in Table 1. The Blob in exposure 1 appears in black (i.e. lower values) while the subsequent positions two, three and four appear as white in the left, middle, and right panel, respectively. The Blob is clearly seen to move towards the top-right corner as the CSM is moved by +1, +1+1, and +4.

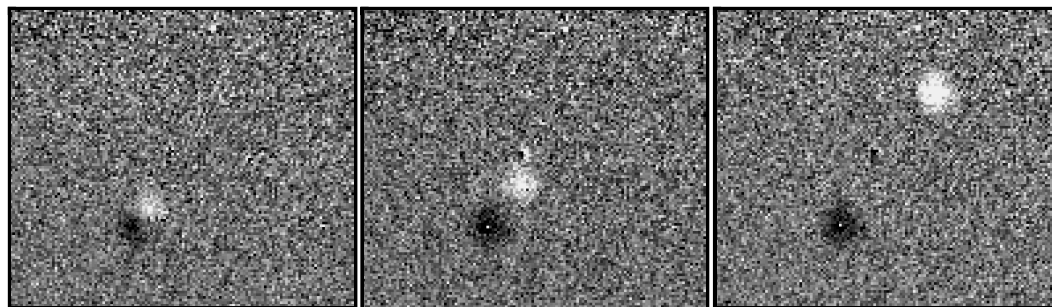
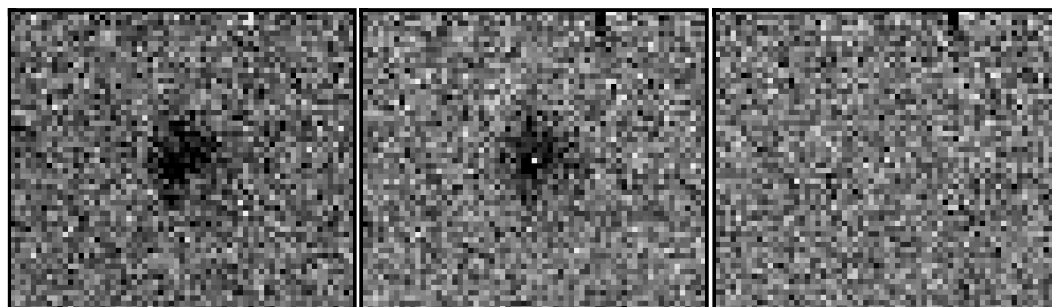


**Figure 4:** A Blob (Blob 1 in Figure 1), as seen in the first (left) and last (middle) exposures of proposal 12006 following the CSM sweeps performed during the course of this proposal. The panel on the right shows the difference between these two exposures, demonstrating that, while we know that the Blob positions correlates with the CSM position, the sources of the Blobs on the CSM mirror remain fixed.



#### 4. Identifying Blobs

As we have discussed above, Blobs are best detected on images with count rates of at least a few 100's of e-/pixel. There are very few fields that have been observed by WFC3 that are sparse enough to provide a uniform illumination of the detector. Many of the available images with high background counts also contain many objects that can mask and hide the presence of a

Blob. We hence have had to rely on combining many deep WFC3 IR observations together in order to construct what can be best thought of as IR sky flats for some of the WFC3 broad filters. Our approach was straight forward and will be further described in an upcoming ISR on generating WFC3 IR sky flats, but goes as follows: First, all of the available high galactic latitude WFC3 IR data in a given filter with integration times greater than 300s and over a given period, usually 30 days long, were identified. In each image, the objects in the field were detected and the SExtractor segmentation map was used to determine the pixels containing light from astronomical sources. The segmentation map was converted into an object mask containing the value of 1 for pixels containing sources and 0 for sky pixels. This mask was then further convolved with a gaussian with  $\sigma=10$  pixels. Following this convolution, pixels with values lower than 0.05 were set to 0 and the remaining pixels were set to 1. Applying this mask to the input image, by avoiding pixels that are masked out, both the median and the mode of the sky pixels were computed and images where the two differed by more than 5% were discarded as not being dominated by background sky (which would tend the whole background level to not be gaussian). Input masked images were then normalized by their median before the set of masked images was combined, on a pixel basis, using a median  $1\sigma$  clipping algorithm. While some of the brighter Blobs are visible in deep single images, as shown in Figure 1, many more are visible in the monthly combined images that we produced, as we demonstrate in Figure 5 where we show F160W sky flat that we generated for the month of February 2010. This sky flat was generated by combining 64 images together and clearly shows the presence of several Blobs, as well as some lower level (1--3% level) flat-fielding residuals.

## 5. Monitoring Blobs

Using IR broad band Sky Flats, like the one shown in Figure 5, over the course of the last few months, we were able to examine Blobs as a function of time. Table 2 summarizes our findings: following the detection of a dozen or so Blobs in the few weeks immediately following SM4, new Blobs appeared at the approximate rate of 1 new Blob per month. This rate appears to have since dropped and no new Blobs have been detected in the last three months. It is hard to estimate the rate of Blob incidence in the first few weeks of WFC3 use because there is not enough data available to construct Sky Flats at this earlier epochs. Except for the individual monitoring and dating of the two largest Blobs shown in Figure 1, we know little of exactly (e.g. within a few weeks) when the most of these Blobs have appeared.

It is to be noted that at no time did we see any of the existing Blobs change in depth or shape or disappear. All Blobs, in all Sky Flats, remain physically static in terms of their positions and shapes. It seems that, at least for now, once a Blob has appeared, it remains a relatively stable artifact in the FOV. Blobs are not observed to grow or become more opaque either. The only thing that has caused the Blobs to apparently move was the CSM not being re-positioned in its default position for the IR channel, as described in the previous section. We also see no correlation between the rate of use of the CSM and the rate of Blob appearance.

**Figure 5:** A F160W Sky Flat generated for the period spanning 02-2010 to 03-2010, generated by combining 64 individually masked WFC3 IR images. Such monthly Sky Flat were used to detect and monitor Blobs in the WFC3 IR channel.

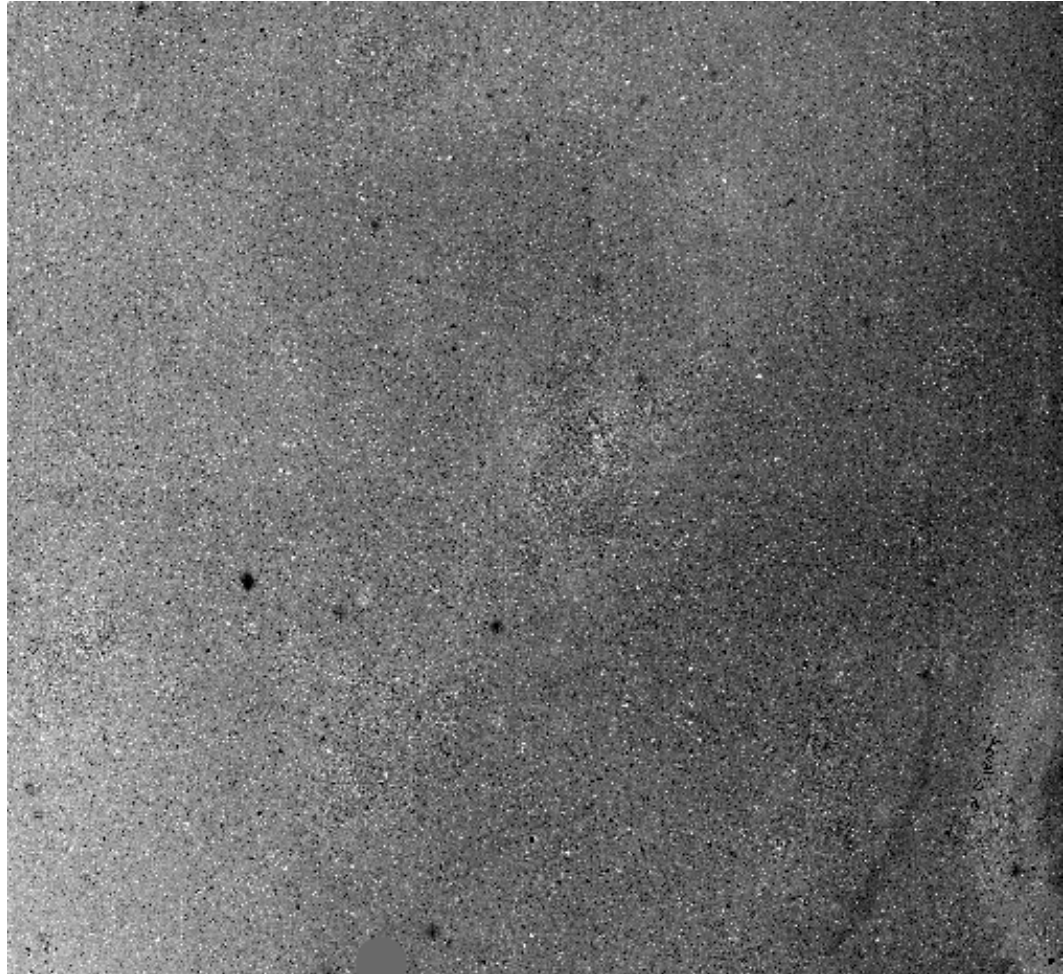


**Table 2:** Cumulative number of Blobs detected in the WFC3 IR channel for the period between September, 2009 and March, 2010. As of the writing of this ISR, the number of new Blobs has recently been observed to decrease and the total number of Blobs has stabilized.

Month	# of Blobs
09/2009	13
10/2009	16
11/2009	17
12/2009	19
01/2010	19
02/2010	19
03/2010	19

## 6. Description and Properties of IR Blobs

We compared the appearance of Blobs in two filters for which we had enough available data to assemble deep Sky Flats images: F125W and F160W. These span the period from December, 2009 to March, 2010 during which the number of Blobs remained unchanged. In Figure 6, we show Blob 1 and Blob 2 (as labeled in Figure 1) as seen in the F125W and F160W data (left and center panel, respectively). We also show the difference between the F125W and F160W data on the rightmost panel. Figure 6 shows that the F125W and F160W data do not subtract out perfectly and that the Blobs seem to be slightly sharper in the F125W than in the F160W band.

Note that we are currently limited to these two bands until more WFC3 data are available to assemble deep Sky Flats using other filters.

We investigated the wavelength dependence of Blobs by measuring their sizes.

It is somewhat difficult to measure the extent of all Blobs in a uniform manner because of their shallowness, and sometimes slow signal to noise or proximity to the edges of the field of view. We hence proceeded to examine the sizes of Blobs using several techniques in both the F125W and F160W bands. We measured their  $x$  light radii ( $R_{50}$ ,  $R_{80}$ , ...,  $R_X$ , which we define as being the radius at which a Blob absorbs 50%, 80%,  $X\%$  of the total light that the Blob absorbs). We also generated azimuthally averaged light profile for each Blob, shown in Figure 7. As shown in this figure, Blobs absorb more light in their central region, with as much as 15--20% absorption in the most affected pixel wide area. We fitted these light profiles to Gaussian profiles and used the results of these fits to estimate  $F_{98}$ , the radius at which the absorption of a particular Blob is less than a 2% effect. We finally attempted to fit each individual Blob using a more generalized two-dimensional Gaussian function. The combination of the last two methods allowed

us, for most Blobs (17 out of 19), to quantitatively estimate the radius at which the absorption of a particular Blob is less than 2%, and that we refer to as F98 in Table 3. Sizes of Blobs that could not be well fitted were visually estimated and are not shown in Table 3.

No strong trend is detected but differences between F125W and F160W data are seen. There is tentative evidence that the Blobs on average appear  $\sim 5\%$  larger and deeper in the F125W band, but these results are marginal at best, as shown in Table 3.

## 7.1 Effect on Photometry and Spectroscopy

The net effect of a typical Blob on stellar photometry is the reduction of the measured flux by 5 to 10%. Observers should be aware of this when designing their observations. It is not clear that Blobs can be properly flattened out using Sky Flats since we see a small wavelength dependence of the physical properties of Blobs. We also have no information on Blobs using anything but the wide band filters F125W and F160W. Narrow and medium band filter observations are not numerous enough and do not typically have background levels high enough to allow us to construct Sky Flats in those bands. Users are advised to circumvent the effect of Blobs by designing their observations to avoid regions affected by Blobs and to sufficiently dither their observations. Using a dither pattern of 20 pixels should be sufficient to avoid the largest of the currently identified Blobs.

Blobs are not directly visible in WFC3 Grism data since these are physically located before the dispersion elements in the instrument's optical path. However, Blobs do affect WFC3 Grism observations as objects falling on or near a Blob will be hidden from the field of view and the Grism. Dithering Grism observations might hence cause an object to be alternatively hidden/attenuated and not hidden in successive slitless observations. In addition to this, the dispersed background is also affected by Blobs as these obscure part of the IR sky. This attenuation of the background (by a few 10's of percent, see Figure 7 and Table 3) is however locally spread out over the whole dispersion length of the Grism elements (just like the rest of the light in slitless observations) and hence should not result in a reduction by more than  $\sim 0.1\%$  of the Grism background. This reduction of the IR background is localized in slitless observations and is limited to a region that is  $\sim 100$  pixel long (the number of pixel the Grism spreads input light over in the first dispersive order) by  $\sim 10$  pixel high (the vertical size of a typical Blob) and that is physically located to the right of the location of a Blob in the field of view.

Table 4 lists the position and size of each of the Blobs currently detected in the IR channel.

## 7.2 Multidrizzle

The Blobs can be a problem for users using Multidrizzle because several of these artifacts are strong enough to significantly affect the final product of Multidrizzle. Users should take care of manually masking the affected areas, shown in Figure 8. We currently flag the affected regions as part of the Data Quality description of the WFC3/IR data with a value of 512. Doing so will al-

low users to relatively easily circumvent the effects of these artifacts when combining multiple images together.

## 8 Future Work

We will continue to monitor WFC3 IR data, on a monthly basis, for the presence of Blobs. As more data become available, we will be able to generate Sky Flats for additional broad band filters and examine Blobs over a larger number of bandpasses. Pixels affected by Blobs will be flagged in the DQ array of pipeline processed WFC3 IR data and the list of such pixels will be updated as new Blobs are identified.

## Conclusion

Following the discovery of small, mostly circular blemishes in deep WFC3 IR images, we have systematically examined every available deep WFC3 IR image. We have determined that the cause of these Blobs is likely material that has been deposited on the CSM mirror that is used to switch incoming light from the UVIS to the IR side of WFC3. About 1.2% of the pixels in the WFC3 IR detector are affected by IR Blobs. This remains a small number of affected pixels compared to the number of known bad and hot pixels.

New Blobs are currently appearing at a slow rate with less than 1 new Blob appearing per month. We have compiled a complete list of these artifacts and, as of the writing of this ISR, there are currently 18 known Blobs in the field of view. Their radii range from a few to ~10 pixels, and the deepest Blobs absorb as much as 15--20% of the light at their center.

Observers wishing to perform accurate photometry are advised to take these artifacts into consideration and to use a dither pattern large enough (~20 pixels) to dither over them.

**Figure 6:** Blobs 1 and 2 as seen in the F125W and the F160W data. The rightmost panel shows the two subtracted. The F125W Blobs are a little sharper and more pronounced than in the F160W filter, causing the subtraction to be imperfect.

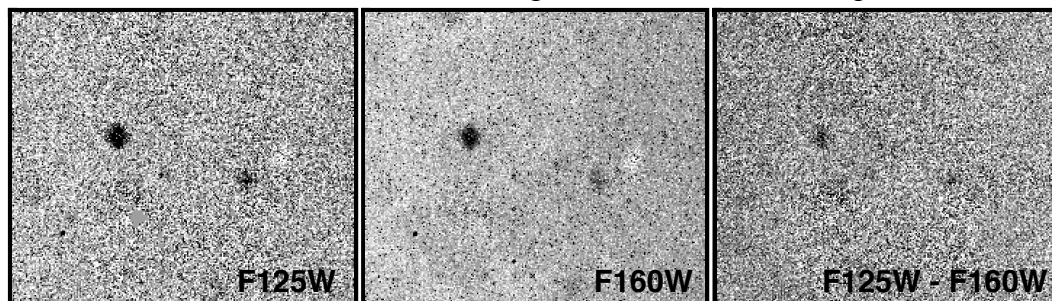


**Figure 7:** The measured light profiles of Blobs in the F125W and F160W Sky Flats. These curves show the fraction of light lost as a function of aperture radius (in pixel). Blobs have a variety of azimuthal profiles and central absorption can be seen to be

as high as ~15--20%.

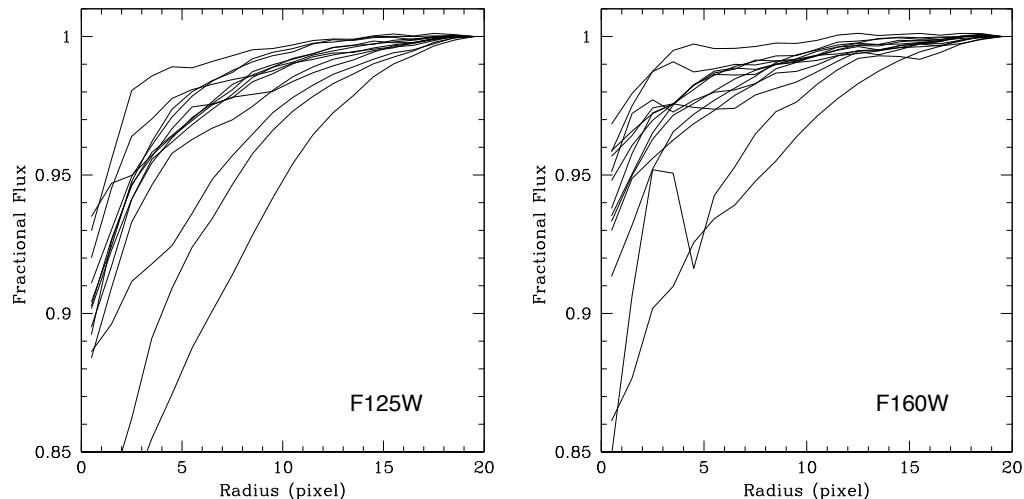


**Table 3:** Summary of the properties of the WFC3 IR Blobs in the F125W and F160W bands that were successfully fitted using a generalized 2D gaussian. This Table lists the half light radius ( $R_a$ , the radius at which a Blob absorbs 50% of the total amount of light it absorbs), the radius at which the absorption from the Blob is less than 2% of the measured background level (F98), and the value (i.e. 1.0-absorption) of the pixel in each Blob where the effect is most pronounced. An unaffected pixel would have a value of 1.0 in this table.

F125W F98	F160W F98	F98 Ratio	F125W $R_{50}$	F160W $R_{50}$	Ratio $R_{50}$	F125W Depth	F160W Depth	Ratio Depth
10.92	9.30	1.17	5.67	1.88	3.01	0.83	0.43	1.92
11.19	1.82	6.16	2.85	2.53	1.12	0.85	0.88	0.97
7.74	6.01	1.29	3.09	3.25	0.95	0.87	0.93	0.94
5.27	6.89	0.77	2.18	2.29	0.95	0.81	0.84	0.96
7.54	7.02	1.07	5.45	3.86	1.41	0.75	0.73	1.02
7.46	2.36	3.16	3.10	2.43	1.27	0.84	0.86	0.98
5.54	3.83	1.45	4.27	4.42	0.97	0.86	0.90	0.95
7.68	12.17	0.63	3.69	2.46	1.50	0.88	0.89	0.98
4.29	5.81	0.74	14.25	16.22	0.88	0.87	0.90	0.97
3.01	2.62	1.15	4.31	8.23	0.52	0.80	0.87	0.91
11.39	11.20	1.02	7.92	5.30	1.49	0.74	0.79	0.94

Instrument Science Report WFC3 2010-06

	F125W F98	F160W F98	F98 Ratio	F125W R <sub>50</sub>	F160W R <sub>50</sub>	Ratio R <sub>50</sub>	F125W Depth	F160W Depth	Ratio Depth
	9.02	10.08	0.89	3.19	3.96	0.80	0.86	0.89	0.96
	7.27	7.70	0.94	5.06	9.73	0.52	0.79	0.85	0.93
	4.48	4.30	1.04	3.94	3.75	1.05	0.73	0.75	0.98
	7.25	8.49	0.85	5.14	4.42	1.16	0.70	0.74	0.94
	12.60	11.91	1.06	8.21	7.91	1.04	0.86	0.90	0.95
	12.73	2.41	5.29	8.86	8.14	1.09	0.85	0.87	0.98
<b>Me- dian</b>	7.54	6.89	1.06	4.31	3.96	1.05	0.84	0.87	0.96
<b>σ</b>	2.97	3.47	1.63	3.01	3.70	0.55	0.06	0.12	0.23

**Table 4:** Position of IR Blobs, their fitted amplitudes, and their approximate sizes (in pixels). As seen in Figure 7, most Blobs affect photometry over a radius of less than ~12 pixels.

x	y	Size (pixel)
128	966	10.0
676	903	7.0
606	874	7.0
863	835	5.0
350	756	10.0
564	699	9.0
822	667	8.0
606	613	8.0
1000	593	8.0
968	572	10.0
228	418	12.0
315	386	9.0
469	376	10.0
877	327	7.0
963	139	8.0
406	81	11.0
864	40	6.0
20	223	10.0
46	7	8.0
	Median	8.00
	$\sigma$	1.77

**Figure 8:** Visual mask showing the location of Blobs in the WFC3/IR field of view as well as their extent, as defined in Table 4.

